A Direct ab Initio Trajectory Study on the Gas-Phase S_N2 Reaction $OH^- + CH_3Cl \rightarrow CH_3OH + Cl^-$

Hiroto Tachikawa,*,† Manabu Igarashi,# and Teruo Ishibashi#

Division of Molecular Chemistry, Graduate School of Engineering, Hokkaido University, Sapporo 060-8628, Japan, and Graduate School of Medicine, Hokkaido University, Sapporo 060-8628, Japan

Received: April 25, 2002; In Final Form: September 12, 2002

Direct ab initio trajectory calculations have been applied to a S_N2 reaction, $OH^- + CH_3Cl \rightarrow CH_3OH + Cl^-$. First, static ab initio molecular orbital (MO) calculations with several basis sets were examined to select the most convenient and best fit basis set to that of high-quality calculations. As a result of the static ab initio calculations, it was found that the Hartree−Fock (HF)/3-21+G(d) calculation reasonably represents a potential energy surface calculated at the MP2/6-311++G(2df,2pd) level. Next, direct ab initio dynamics calculations using the 3-21+G(d) basis set were carried out for the S_N2 reaction. A full dimensional potential energy surface including all degrees of freedom was used in the dynamics calculation. The collision energies chosen were $E_{coll} = 5$ and 25 kcal/mol. In the collisions at $E_{coll} = 5$ and 25 kcal/mol, 48% and 63% of the total available energies were, respectively, partitioned into the relative translational mode between CH_3OH and Cl^-. Also, it was predicted that the C−H stretching mode of the product CH_3OH is excited after the S_N2 reaction, which is not detected in the case of the halogen-atom exchange S_N2 reaction. The reaction mechanism was discussed on the basis of theoretical results.

1. Introduction

Bimolecular nuclear substitution (S_N2) reactions of a type $X^- + CH_3Y \rightarrow CH_3X + Y^-$ are one of the fundamental organic reactions and have been studied extensively from both experimental and theoretical points of view.[1,2] In particular, halogen exchange reactions (X and Y = halogen atoms) are simplest in the S_N2 reactions. Therefore, much work has been carried out.[1−4]

For the reaction dynamics of the halogen exchange S_N2 reaction, Hase and co-workers have done extensive investigations by means of classical trajectory method with ab initio fitted analytical potential energy functions.[3] Several characteristic features for the halogen exchange S_N2 reactions have been elucidated from their results. Although the dynamics of the halogen exchange reactions were thus known theoretically,[3,4] the mechanism of the S_N2 reactions of molecular ions (such as OH^- and CH_3O^- ions) was not clearly understood. This is because dimension, which should be included in the calculation, will increase greatly as the number of atoms in the reaction system is increased. Therefore, the procedure of the fitting becomes more difficult and more complicated.

In the present study, we have investigated a S_N2 reaction of molecular ion OH^- with CH_3Cl,

$$OH^- + CH_3Cl \rightarrow CH_3OH + Cl^- \qquad (I)$$

by means of direct ab initio trajectory method. In this method, we do not need a fitting procedure of PES to an analytical function. Therefore, it is suitable to investigate a complex S_N2 reaction using direct ab initio trajectory methods. In a previous paper, we have made direct ab initio dynamics calculations for the similar S_N2 reactions $F^-(H_2O)_n + CH_3Cl$ ($n = 0, 1$).[5−8] Mechanism, collision energy dependence, and branching ratios of the product channels were all predicted from the calculations. Also, it was suggested that direct ab initio trajectory method is a powerful tool to investigate the reaction dynamics for the reactions with large degrees of freedom.

Reaction I has been investigated extensively by several experimental techniques: selected ion flow tubes (SIFT) at 300 K,[9,10] double mass spectrometer at relative energies down to 0.3 eV,[11] flowing after glow technique,[12,13] and pulsed ion cyclotron resonance (ICR) spectroscopy.[14] The reaction rate was measured to be $(13−16) \times 10^{-10}$ cm^3 mol^{-1} s^{-1} at 300 K (estimated accuracy is 50%). Temperature dependence on the reaction rate[15] was also measured by Hierl et al. in the temperature range 200−500 K. They suggested that the reaction rate decreases with increasing temperature. Also, the branching ratios of the product channels were measured for the very similar S_N2 reaction $OH^- + CH_3Br$.[10]

From a theoretical point of view, Morokuma and Ohta[16] investigated the potential energy diagram for reaction I by means of ab initio molecular orbital (MO) calculations. Their calculations indicated that there are double minima corresponding to pre- and late-complexes, while the transition state is lower in energy than the initial separation. Recently, they carried out more accurate ab initio calculations for reaction I and obtained a more accurate potential energy diagram.[17] The similar features were obtained by Evanseck et al.[18] For reaction I, static ab initio MO calculations have been thus carried out by several authors.[16−19] However, there is no dynamics study for reaction I because the reaction has many degrees of freedom ($3N - 6 = 15$, where N is number of atoms in the reaction system).

In the present paper, we have first examined ab initio MO calculations with several basis sets for reaction I. The most reasonable basis set to represent the potential energy surface was determined by means of static ab initio MO calculations.

* To whom correspondence should be addressed. E-mail: hiroto@eng.hokudai.ac.jp. Fax: +81 11706-7897.
† Graduate School of Engineering.
# Graduate School of Medicine.

10.1021/jp0210632 CCC: $22.00
Published on Web 10/18/2002

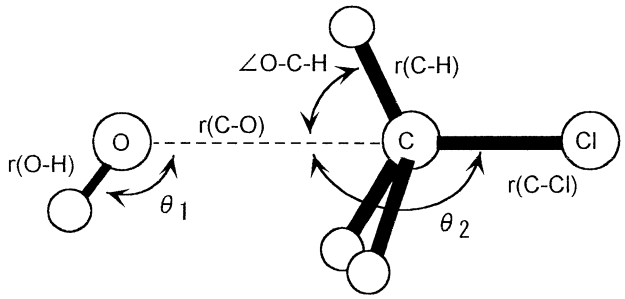

Figure 1. Geometrical parameters for the reaction system $OH^- + CH_3Cl$.

Second, direct ab initio trajectory calculations were carried out for reaction I using the selected basis set. The dynamics and energy partitioning in reaction I were discussed on the basis of theoretical results. Note that this work is the first study to investigate dynamics of reaction I.

2. Methods of the Calculations

All static ab initio MO calculations were carried out using the Gaussian 98 program package.[20] A range of different basis sets were tested from split valence plus polarization 3-21G(d) to large and flexible sets such as 6-311++G(2df,2pd) with sets of polarization functions. Also considered were Dunning basis sets D95++(d,p).

By using the most reasonable basis set determined by the ab initio MO calculations [it is the 3-21+G(d) basis set], we have carried out direct ab initio trajectory calculations[21−25] for reaction I. The Hartree−Fock (HF)/3-21+G(d) optimized geometry of CH_3Cl was chosen as an initial structure. At the start of the trajectory calculation, atomic velocities of CH_3Cl were adjusted to give a mean temperature of 10 K. Temperature of the reaction system is defined by

$$T = \frac{1}{3kN}\left\langle \sum_i m_i v_i^2 \right\rangle \tag{1}$$

where N is number of atoms, v_i and m_i are velocity and mass of the ith atom, and k is Boltzmann's constant.

Figure 1 shows the structure and geometrical parameters of the reaction system. At initial separations, that is, $OH^- + CH_3Cl$, the angles of H−O−CH_3Cl (θ_1) were randomly generated from 0.0° to 180°. The distances between OH and CH_3Cl, r(C−O), were also generated within 8.0−10.0 Å. The impact parameter (b) was selected to be near zero in the present calculations ($b = 0.0 \pm 0.1$ Å). A total of 73 geometrical configurations were randomly generated, and 73 trajectories are run for each collision energy (E_{coll}). We choose two collision energies $E_{coll} = 5.0$ and 25.0 kcal/mol. The equations of motion for n atoms in the reaction system are given by

$$\frac{dQ_j}{dt} = \frac{\partial H}{\partial P_j}$$

$$\frac{\partial P_j}{\partial t} = -\frac{\partial H}{\partial Q_j} = -\frac{\partial U}{\partial Q_j} \tag{2}$$

where $j = 1-3N$, H is the classical Hamiltonian, U is the potential energy of the reaction system, Q_j is the Cartesian coordinate of jth mode, and P_j is the conjugated momentum. These equations were numerically solved by the standard fourth-order Runge−Kutta and sixth-order Adams−Moulton combined algorithm. No symmetry restriction was applied to the calculation of the gradients (i.e., positions of the atoms H−O−C−Cl of the reaction system were not restricted to a plane). The time step size was chosen as 0.2 fs, and a total of 5000 steps were integrated for each dynamics calculation. The drift of the total energy is confirmed to be less than 2% at all steps in the trajectory. Rotational quantum number of OH^- at initial separation was assumed to be zero ($J = 0$).

To estimate the effect of the impact parameter on the reaction dynamics, 30 trajectories with nonzero impact parameters were preliminary tested. The maximum of the impact parameter (b_{max}) was obtained, and the effect of the impact parameter was discussed.

TABLE 1: Total Energies (in au) and Reaction Energies (ΔE in kcal/mol) for $OH^- + CH_3Cl \rightarrow CH_3OH + Cl^-$ Reaction System

method	$OH^- + CH_3Cl$	$Cl^- + CH_3OH$	$-\Delta E$
HF/3-21G*	−571.663 626 0	−571.842 138 9	112.0
HF/3-21+G*	−571.796 924 4	−571.894 392 0	61.2 (56.5)[a]
HF/6-31G*	−574.419 751 0	−574.561 415 0	88.9
HF/6-31+G*	−574.470 581 7	−574.580 626 1	69.1
HF/6-31++G**	−574.483 141 8	−574.592 175 2	68.4
HF/D95*	−574.456 479 0	−574.567 532 1	69.7
HF/D95+*	−574.488 251 2	−574.600 101 9	70.2
HF/D95**	−574.467 647 7	−574.578 423 7	69.5
HF/D95++**	−574.500 894 5	−574.611 276 7	69.3
MP2/6-311++G(d,p)	−575.069 047 7	−575.148 155 5	49.6
MP2/6-311++G(df,pd)	−575.142 729 0	−575.221 684 0	49.6
MP2/6-311++G(2df,2pd)	−575.193 210 0	−575.274 276 1	50.9
$\Delta H°$ (exptl)[b]			(50)

[a] ΔH calculated is given in parentheses. [b] Experimental value for heat of reaction cited from ref 26.

3. Results and Discussion

3.1. Ab Initio MO Study. One of the important factors dominating in reaction dynamics would be a reaction energy (ΔE) or a heat of reaction ($-\Delta H$). Therefore, the total energies for the reactant and products, $OH^- + CH_3Cl \rightarrow CH_3OH + Cl^-$, were calculated by several methods. The results were given in Table 1. The ΔE's calculated by the HF level of theory with several basis sets were distributed in the range 61.2−112.0 kcal/mol, which are larger than that of the MP2/6-311++G(2df,-2pd) calculations (50.9 kcal/mol). However, it seems that the HF/3-21+G(d) calculation gave a relatively reasonable value (61.2 kcal/mol). The heat of reaction calculated at the HF/3-21+G(d) level was $-\Delta H = 56.5$ kcal/mol, which is reasonable agreement with the experimental value (50 kcal mo1^{-1}).[26] The agreement of the 3−2l+G(d) basis set with experimental values was attributed to the fact that the diffuse functions added to the oxygen and halogen atoms (OH^- and Cl^-) cause an energy reduction.

The relative energies (E_{rel}) and geometries at the stationary points along the reaction coordinate calculated at the HF/3-21+G(d) and MP2/6-311++G(2df,2pd) levels were summarized in Table 2. It should be noted that MP2/6-311++G-(2df,2pd) calculation gives reasonable geometries and energies for several S_N2 reactions.[7,8,16,17] Therefore, it is meaningful to compare with the values calculated by the HF/3-21+G(d) level. The zero level in E_{rel} corresponds to the energy of the reactant ($OH^- + CH_3Cl$). It was found that the energies for the early- and late-intermediate complexes calculated by HF/3-21+G(d) are in excellent agreement with those of MP2 calculations with the 6-311++G(2df,2pd) basis set. In addition, the energy of the saddle point was also in good agreement between the two, although the HF calculation gave a slightly lower value (−16.5 vs −12.9 kcal/mol). As is clearly indicated in Table 2, the HF/

TABLE 2: Ab Initio Geometries and Relative Energies (E_{Rel} in kcal/mol) for Stationary Points on the Reaction Path[a]

	r(C−O)	r(C−Cl)	r(C−H)	∠Cl−C−H	∠H−C−H	E_{rel}
			$OH^- + CH_3Cl$ Reactants			
HF/3-21+G(d)	∞	1.806	1.076	108.2	110.7	0.0
MP2/6-311++G(2df,2pd)	∞	1.778	1.083	108.6	110.3	0.0
			$HO^{-}\cdots CH_3Cl$ Complex			
HF/3-21+G(d)	2.567	1.908	1.067	106.5	112.2	−17.8
MP2/6-311++G(2df,2pd)	2.586	1.823	1.078	108.7	110.1	−15.9
			$[HO\cdots CH_3\cdots Cl]^-$ Saddle Point			
HF/3-21+G(d)	2.287	2.090	1.060	99.8	117.1	−16.5
MP2/6-311++G(2df,2pd)	2.192	2.040	1.070	99.1	117.6	−12.9
			$HOCH_3\cdots Cl^-$ Complex			
HF/3-21+G(d)	1.443	3.720	1.080		109.4	−74.8
MP2/6-311++G(2df,2pd)	1.400	3.480	1.090		108.0	−68.8
			$HOCH_3 + Cl^-$ Products			
HF/3-21+G(d)	1.455	∞	1.081	67.4	109.2	−60.7
MP2/6-311++G(2df,2pd)	1.421	∞	1.088	69.7	108.6	−50.9

[a] Bond lengths and angles are in Å and in deg, respectively.

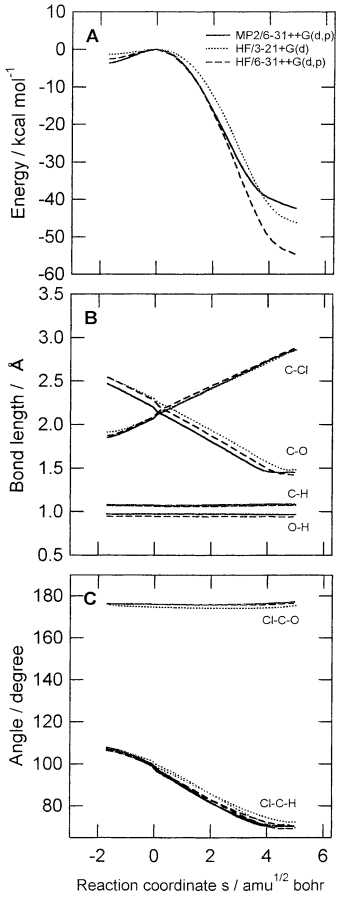

Figure 2. Potential energy of the reaction system and geometrical parameters plotted as a function of intrinsic reaction coordinate (IRC) for the reaction $OH^- + CH_3Cl \rightarrow CH_3OH + Cl^-$, calculated at the several levels of theory.

3-21+G(d) calculations for geometries and relative energies at the stationary points represent reasonably those of the most sophisticated calculations.

To compare the curvature and geometrical change around the saddle point in more detail, intrinsic reaction coordinates (IRCs) were calculated by several methods. The results were given in Figure 2. The calculations were carried out at the HF/3-21+G(d), HF/6-31++G(d,p), and MP2/6-31++G(d,p) levels of theory. As is shown in Figure 2A, the energy calculated by HF/3-21+G(d) was close to that of the MP2 calculation, although the curvature has swollen slightly. This is because the HF/3-21+G(d) calculation was somewhat underestimated for imaginary frequency of the saddle point (370i vs 536i cm^{-1}). The geometrical parameters along IRC (Figure 2B,C) were in good agreement with those of the MP2 calculation.

At a point in the entrance region of the reaction ($s = -2.0$ $amu^{1/2}$ bohr), potential energy curve (PEC) along the angle ∠H−O−C (θ_1) were calculated at both HF and MP2 levels. Both levels of theory gave similar results and indicated that the angle θ_1 has the minimum at $\theta_1 = 180°$ and the maximum at $\theta_1 = 0°$. The shape of PEC was very shallow in the region $\theta_1 = 90-180°$. However, the energy of the barrier becomes higher in the smaller angles ($\theta_1 = 0-50°$). This implies that the OH^- ion approaching to CH_3Cl can rotate freely at longer separation but the orientation of OH^- relative to CH_3Cl is slightly restricted at shorter distance from CH_3Cl.

The harmonic vibrational frequencies for the molecules at the stationary points are given in Table 3. The negative frequencies at the transition state were calculated to be 536i (MP2) and 370i cm^{-1} (HF), indicating that the HF calculation gives a looser saddle point. However, the other modes calculated by the HF calculation are in reasonable agreement with those of the MP2 calculation, although the HF calculation gives slight larger values. The frequencies for the C−O and C−H stretching modes of the product CH_3OH were calculated by the HF calculation to be 1050 and 3206−3290 cm^{-1}, respectively. These values are close to the experimental (1033 and 2844−3000 cm^{-1}) and MP2 values (1055 and 3065−3166 cm^{-1}).

These results indicate strongly that the HF/3-21+G(d) calculation would give a reasonable multidimensional potential energy surface (PES) for the S_N2 reaction $OH^- + CH_3Cl \rightarrow CH_3OH + Cl^-$. At the very least, this level of theory is applicable to a qualitative argument for reaction I.

3.2. Direct ab Initio Trajectory Study. As indicated by the static ab initio MO calculations with several basis sets, the HF/3-21+G(d) calculation gave a reasonable PES for reaction I. In this section, we shall attempt direct ab initio trajectory calculations for the S_N2 reaction at the HF/3-21+G(d) level. Two center-of-mass collision energies ($E_{coll} = 5$ and 25 kcal/mol) were chosen, and a total of 73 orientations of OH^- relative to CH_3Cl were examined at each collision energy. Rotational quantum number of OH^- was assumed to be zero. Here, two typical sample trajectories were shown and discussed: one is that the oxygen atom of OH^- orients toward the carbon of CH_3Cl at initial separation (i.e., the angle of H−O−C is close to 180°), and the other one is that the hydrogen of OH^- directs to CH_3Cl (i.e., the angle is close to 0°).

TABLE 3: Harmonic Vibrational Frequencies (cm^{-1}) of the Stationary Points at the HF/3-21+G(d) and MP2/6-311++G(d,p) Levels[a]

stationary point	assignment	HF	MP2
saddle point $[HO\cdots CH_3\cdots Cl]^-$	HO−C−Cl asym str	370i	536i
	OH str	3742	3849
	CH_3 str	3562	3409
	CH_3 str	3561	3406
	CH_3 str	3383	3213
	CH_3 deform	1561	1414
	CH_3 deform	1558	1408
	CH_3 deform	1324	1144
	CH_3 rock	1069	1009
	CH_3 rock	1050	985
	OH bend	335	513
	HO−C−Cl sym str	278	293
	HO−C−Cl bend	219	229
	HO−C−Cl bend	200	218
	torsion	76	58
late-complex $[HOCH_3\cdots Cl^-]$	OH str	3624	3402
	CH_3 str	3252	3115
	CH_3 str	3231	3086
	CH_3 str	3184	3023
	CH_3 deform	1676	1538
	CH_3 deform	1660	1505
	CH_3 deform	1602	1496
	OH bend	1508	1487
	CH_3 rock	1253	1199
	CH_3 rock	1181	1146
	C−O str	1094	1112
	HO−C···Cl bend	771	799
	$CH_3OH\cdots Cl$ str	175	209
	$CH_3OH\cdots Cl$ bend	101	111
	torsion	84	69
product $HOCH_3 + Cl^-$	OH str	3889	3922 (3681)
	CH_3 str	3290	3166 (3000)
	CH_3 str	3265	3140 (2960)
	CH_3 str	3206	3063 (2844)
	CH_3 deform	1668	1530 (1477)
	CH_3 deform	1667	1520 (1477)
	CH_3 deform	1613	1511 (1455)
	OH bend	1407	1379 (1345)
	CH_3 rock	1264	1202 (1165)
	CH_3 rock	1118	1113 (1060)
	C−O str	1050	1055 (1033)
	torsion	265	276 (295)

[a] Experimental values cited from ref 28 are given in parentheses.

A. Sample Trajectory 1. Snapshots. Snapshots calculated for the oxygen oriented toward the carbon atom at initial separation were illustrated in Figure 3. In this trajectory, the initial separation between the OH^- ion and the carbon atom of CH_3Cl was chosen as r(C−O) = 9.942 Å, and the angles of H−O−C and O−C−Cl, θ_1 and θ_2, were 177.9° and 179.9° at time zero, respectively. The center of mass collision energy at the initial point was 5.0 kcal/mol. At time 0.25 ps, OH^- approached CH_3Cl at r(C−O) = 5.433 Å, but the H−O−C angle (θ_1) was not changed, and it was still 179.6°. At 0.347 ps, the OH^- ion was located at 2.726 Å far from the carbon atom of CH_3Cl, which is enough to interact strongly as ion−dipole complex. The stabilization energy of the complex at this point was 17 kcal/mol relative to the initial separation. After that, a Walden inversion of the methyl group takes place around time t = 0.374 ps, while a Cl−C−H angle of the methyl group was close to 90°. This structure corresponds to transition state (TS) in the S_N2 reaction. At time t = 0.416 ps, the methanol molecule, which is bound weakly to the Cl^- ion, was formed. This complex corresponds to the late complex in the S_N2 reaction. This complex decomposed to CH_3OH and Cl^- at 0.50 ps because of the excess energy formed by the ion exchange reaction.

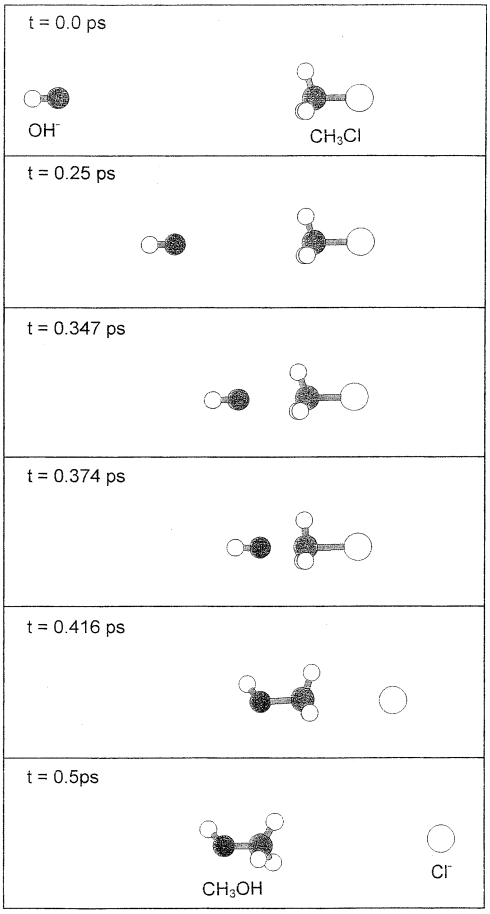

Figure 3. Snapshots of the conformations for the sample trajectory illustrated as a function of reaction time. Initial parameters are the distances r(C−O) = 9.942 Å, r(O−H) = 0.978 Å, and r(C−Cl) = 1.760 Å and angles θ_1 = 177.9°, θ_2 = 179.9°, and ∠O−C−H = 70.5° (namely, the oxygen oriented toward the carbon atom). Center of mass collision energy (E_{coll}) is 5.0 kcal/mol. The 3-21+G(d) basis set was used for $CH_3Cl + OH^-$.

Potential energy of the reaction system. To elucidate the reaction dynamics of OH^- with CH_3Cl in more detail, time dependence of the potential energy of the reaction system (PE), intra- and intermolecular distances, and angles were plotted in Figure 4. This trajectory corresponds to that given in Figure 3. PE plotted as a function of reaction time was given in Figure 4A. Part B of Figure 4 indicates the intermolecular distances r(C−Cl) and r(C−O). Parts C and D indicate the bond distances (r(C−H) and r(O−H)) and angles (θ_1, θ_2, and ∠OCH), respectively.

After the start of the reaction, PE decreased gradually as a function of reaction time, and it reaches −17.6 kcal/mol at time 0.36 ps. This energy minimum corresponds to the precomplex composed of HO^-−CH_3Cl, which is an ion−dipole complex. During this approach, the r(C−O) deceased almost linearly as a function of reaction time, and then OH^- collided with the carbon of CH_3Cl at time = 0.38 ps. The lifetime of the complex HO^-−CH_3Cl was very short (τ < 10 fs), and the trajectory rapidly entered into the transition state (TS) region. In the case of this sample trajectory, the dynamical barrier height at the TS was calculated as 0.5 kcal/mol relative to the initial separation. After passing the TS region, PE decreased suddenly to −57 kcal/mol at 0.42 ps, and then it increased gradually to −50 kcal/mol at 0.80 ps. The trajectory reached the product region at time t = 1.0 ps.

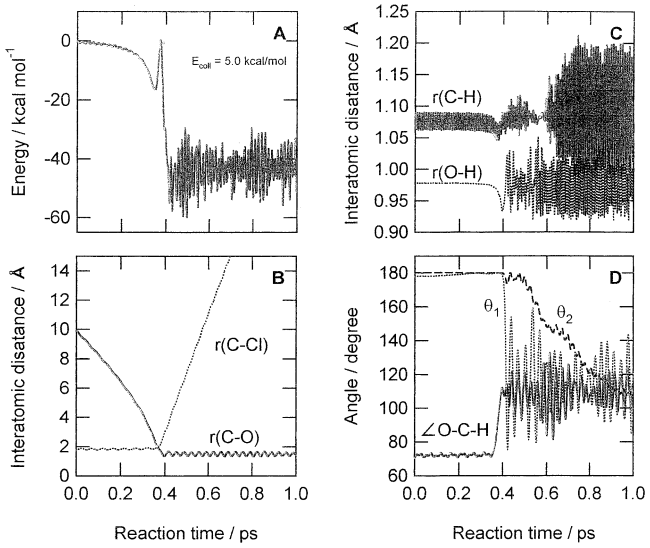

Figure 4. Results as a function of reaction time of the sample trajectory: (A) potential energy of the system; (B) interatomic distances; (C) intraatomic distances; (D) angles. Initial condition of the trajectory calculation is the same as that in Figure 3.

Figure 4B shows time dependence of bond distances, r(C−Cl) and r(C−O). The bond breaking and formation processes were clearly shown in this figure. In the course of the S_N2 reaction, the intermolecular distance r(C−O) decreased as reaction time is increased. At time 0.374 ps, the C−O distance was crossed to that of C−Cl distance, meaning that the bond exchanges took place in this region. However, the C−O stretching mode of CH_3OH formed by the exchange reaction was in the ground state. Figure 4C showed time-dependence of the C−H stretching of CH_3Cl and the O−H stretching modes of CH_3OH. Before TS, the C−H stretching mode was in the ground state (the amplitude was 0.03 Å). After TS, the O−H vibrational mode was vibrated in the range 0.93−1.02 Å (the amplitude was 0.09 Å), while the C−H stretching mode was slightly enhanced in the time region 0.4−0.6 ps (the amplitude was 0.06 Å). At time 0.60 ps, the vibrational mode for the C−H stretching of CH_3OH was excited because the energy transfer from the O−H stretching mode to the C−H stretching mode occurs efficiently by an internal mode coupling in CH_3OH (the amplitude of the C−H mode was 0.204 Å). This feature was clearly seen in Figure 4C as the change of amplitudes. This was also seen in the time dependence of angles (θ_1 and ∠O−C−H) as shown in Figure 4D.

B. Sample Trajectory 2. Snapshots. The similar dynamics calculation was also carried out for the hydrogen orientation form at the initial separation (i.e., the angle H−O−C is close to zero). Snapshots calculated for the hydrogen oriented toward the carbon atom at initial separation were illustrated in Figure 5. In this trajectory, the initial separation between the OH^- ion and the carbon atom of CH_3Cl was chosen as r(C−O) = 9.947 Å, and the angles of H−O−C and O−C−Cl, θ_1 and θ_2, were 3.2° and 179.4° at time zero, respectively. The center of mass collision energy at the initial point was 5.0 kcal/mol.

At time 0.25 ps, OH^- approached CH_3Cl at r(C−O) = 5.533 Å, and the H−O−C angle (θ_1) was significantly changed to 38.4°. At 0.356 ps, the OH^- ion was located at 2.644 Å from the carbon atom of CH_3Cl, which is enough to interact strongly as ion−dipole complex. The stabilization energy of the complex at this point was 18 kcal/mol relative to the initial separation. After that, a Walden inversion of the methyl group took place around time t = 0.39 ps, while a Cl−C−H angle of the methyl group was close to 90°. A methanol molecule was formed at 0.476 ps.

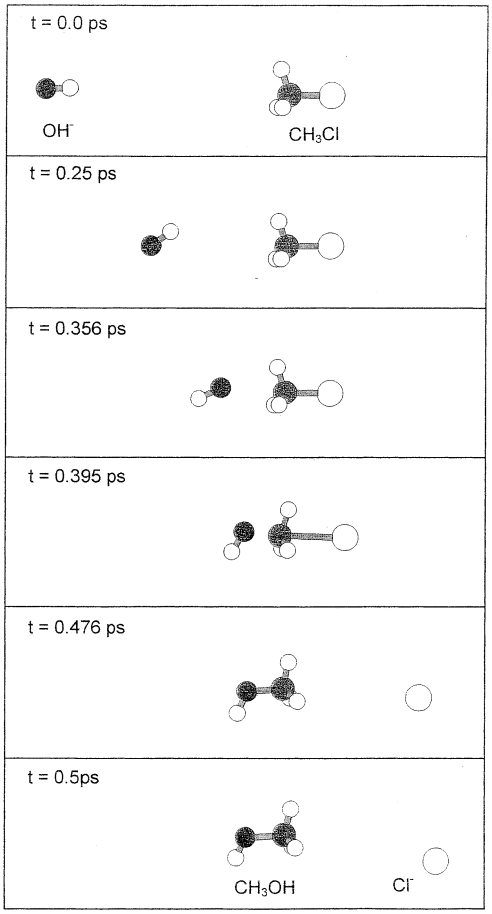

Figure 5. Snapshots of the conformations for the sample trajectory illustrated as a function of reaction time. Initial parameters are the distances r(C−O) = 9.947 Å, r(O−H) = 0.978 Å, and r(C−Cl) = 1.761 Å and angles θ_1 = 3.2°, θ_2 = 179.4°, and ∠O−C−H = 69.9° (namely, the hydrogen oriented toward the carbon atom). Center of mass collision energy (E_{coll}) is 5.0 kcal/mol.

Potential energy of the reaction system. The PE, intra- and intermolecular distances, and angles were plotted in Figure 6. This trajectory corresponds to that given in Figure 6. After starting the reaction, PE decreased gradually as a function of reaction time, and it reaches −18.0 kcal/mol at time 0.36 ps at which the energy minimum corresponds to the precomplex composed of HO^-−CH_3Cl. The lifetime of the complex HO^-−CH_3Cl was very short (τ < 5 fs) After passing TS, PE decreased suddenly to −62.0 kcal/mol, and the energy vibrated rapidly in the range −60 to −18 kcal/mol. From time dependence of bond distances (Figure 6B), it was found that the substitution occurs at time t = 0.38 ps, and the C−O stretching mode was excited. Also, the C−H and O−H bonds were fluctuated after the substitution. For this sample trajectory, total available energy was almost partitioned into the internal modes of CH_3OH. About 35% of the total available energy was dissipated into the translational energy. The C−O stretching mode was significantly more excited for this sample trajectory with the oxygen oriented toward the carbon.

C. Distributions of Relative Translational Energies. Populations for the relative translational energies between CH_3OH and Cl^- formed by reaction I, calculated from all trajectories (146 trajectories), were plotted in Figure 7. For a lower collision energy, E_{coll} = 5 kcal/mol, population was distributed widely from 21 to 36 kcal/mol with a peak at 31 kcal/mol. Also, the

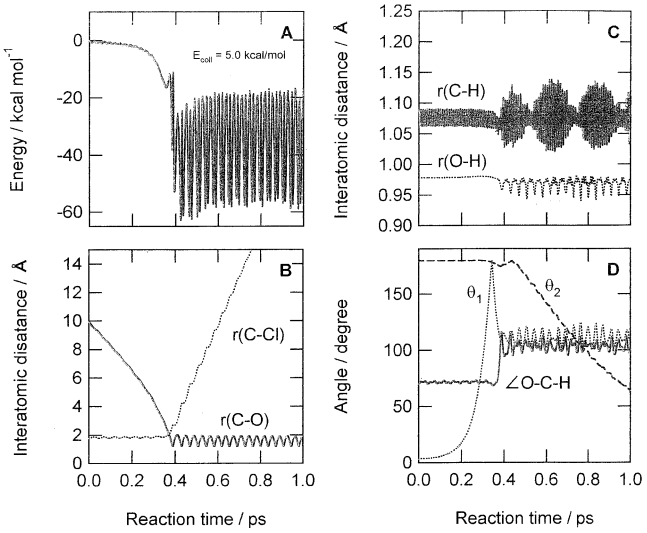

Figure 6. Results as a function of reaction time of the sample trajectory for the hydrogen orientation form: (A) potential energy of the system; (B) interatomic distances; (C) intraatomic distances; (D) angles. Initial condition of the trajectory calculation is the same as that in Figure 5.

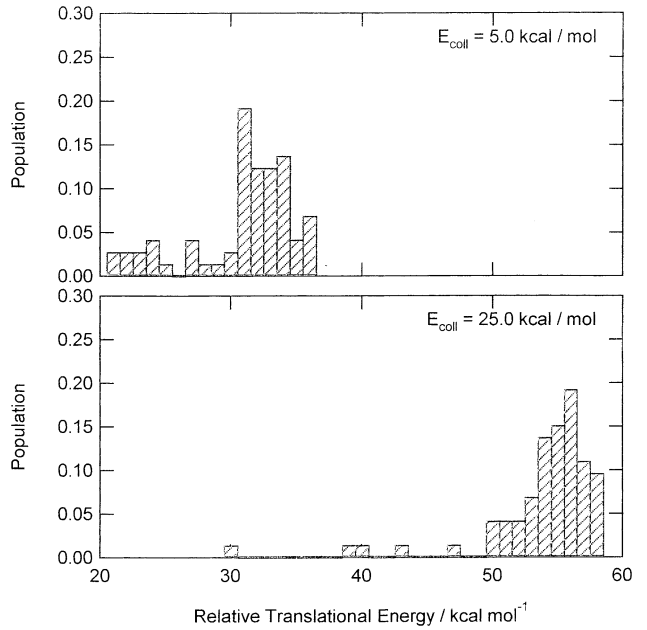

Figure 7. Populations of relative translational energy between products, CH_3OH and Cl^-, obtained by direct ab initio trajectory calculations. Collision energies are 5 (upper) and 25 kcal/mol (lower). A total of 146 trajectories were run.

distribution has a long tail in the range 21−28 kcal/mol. The peak of population moved to 56 kcal/mol at E_{coll} = 25 kcal/mol. At this collision energy, population has also a long tail for lower energy region. From analysis of the initial separation, it was found that the long tails are formed mainly by the collision with the hydrogen oriented toward the carbon atom. In this report, angular distributions were not given because of trajectories as near-zero impact parameter.

D. Effect of Impact Parameter on the Reaction Dynamics. The present calculations were carried out on the assumption of near-zero impact parameter ($b = 0.0 \pm 0.1$ Å) to keep a realistic CPU time. However, the actual reaction occurs as random collisions in the gas phase. In this section, therefore, to elucidate the effect of impact parameter on the reaction dynamics, we preliminarily calculated trajectories with nonzero impact parameters. First, we determined roughly the maximum of the

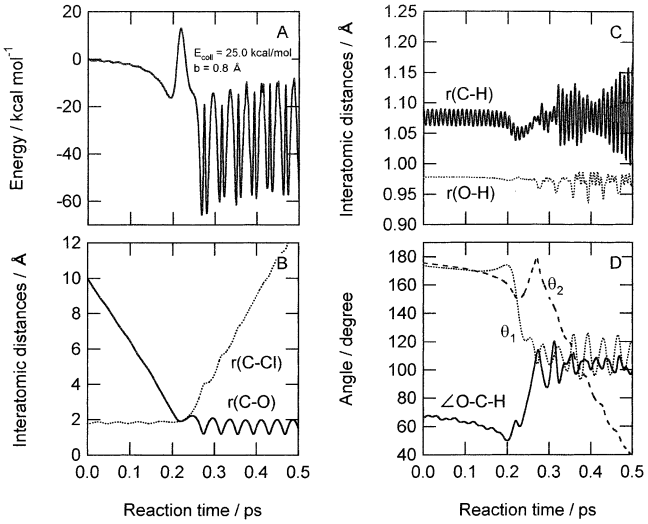

Figure 8. Results as a function of reaction time of the sample trajectory for a collision with large impact parameter: (A) potential energy of the system; (B) interatomic distances; (C) intraatomic distances; (D) angles. Initial parameters are $b = 0.8$ Å, the distances r(C−O) = 10.01 Å, r(O−H) = 0.978 Å, and r(C−Cl) = 1.760 Å, and angles θ_1 = 176.8°, θ_2 = 179.8°, and ∠O−C−H = 1.0° (the oxygen oriented toward the carbon atom). Center of mass collision energy (E_{coll}) is 25.0 kcal/mol. The 3-21+G(d) basis set was used for $CH_3Cl + OH^-$.

impact parameter (b_{max}) at E_{coll} = 25 kcal/mol. Five trajectories were calculated for each impact parameter with 0.2−1.2 Å (interval is 0.20 Å). From the calculations, b_{max} was obtained as 1.0 Å.

Figure 8 shows the result of the trajectory calculation with b = 0.8 Å at E_{coll} = 25 kcal/mol. This trajectory would be a sample of collisions with larger impact parameters. The OH^- ion started at time zero from 10.0 Å from CH_3Cl as the r(C−O) distance. The precomplex [$HO^-\cdots CH_3Cl$] was formed at time t = 0.2 ps. After the transition state, the energy vibrated strongly as a function of time. The C−H and O−H bond distances are plotted in Figure 8C. The amplitude of the C−H bond is ca. 0.03 Å before the transition state, whereas it increased suddenly to 0.10−0.12 Å after Walden inversion. This feature is similar to that given as b = 0.0 Å in Figure 4, although the amplitude for b = 0.8 Å is slightly larger than that for b = 0.0 Å. The relative translational energy between Cl^- and CH_3OH for this sample trajectory was calculated to be 35.6 kcal/mol, which is 41.4% of the total available energy. These results strongly indicated that the collision with larger impact parameter increases internal energy of the product CH_3OH molecule.

4. Discussion

A. Summary. In the present study, first, we have examined several basis sets for the energetics, relative energies, and geometrical configurations along the reaction coordinate of a S_N2 reaction $OH^- + CH_3Cl \rightarrow CH_3OH + Cl^-$ (reaction I). It was obtained from the static ab initio MO calculations that the HF/3-2l+G(d) calculation gives a reasonable potential energy surface for reaction I. CPU time for the dynamics calculation with this basis set is significantly shorter than those for the other basis sets such as 6-311++G(d,p). Therefore, the HF/3-21+G(d) level of theory is suitable and convenient for calculating the reaction dynamics.

Next, direct ab initio trajectory calculations were carried out for reaction I using 3-21+G(d) basis set. The dynamics calculations showed that the title S_N2 reaction occurs mainly by direct mechanism: namely, the trajectory passes quickly

through the complex regions (pre- and late-complex regions). This is because the reaction energy is significantly large (about 50 kcal/mol) and also the basins of the complex regions are shallow for the product channel. Therefore, almost trajectories proceed via direct mechanism. The initial angle of OH relative to the CH_3Cl molecule slightly affects the lifetime of the complexes, but its angle dependency on the lifetime was negligibly small. The angle mainly causes a slight change of the internal energy.

The relative translational energies (E_{rel}) increased with increasing collision energy (E_{coll}); for example, relative translational energies at $E_{coll} = 5$ and 25 kcal/mol were calculated to be 31.4 and 54.0 kcal/mol, respectively. These energies correspond to 48% and 63% of total available energy of the reactions. At low collision energy ($E_{coll} = 5$ kcal/mol), half of the total available energy was partitioned into the internal energy of CH_3OH. The averaged translational energy calculated as 54 kcal/mol is slightly larger than the expected value (31.4 + 25.0 kcal/mol). This may be caused by statistical error because of a limited number of trajectories.

The effect of the impact parameter was preliminary examined in the present calculations. The calculations showed that the energy transfer from total available energy to the internal modes of the product CH_3OH is more effective in the case of large impact parameters than that of zero-impact parameter. This is because the bending mode of HO−C−Cl would be coupled effectively with the C−H stretching mode of methyl group for the trajectory with a large impact parameter.

B. Comparison with Previous Studies. In previous papers,[5−8] we investigated halogen-atom exchange reactions $F^- + CH_3Cl$. In this reaction, the excess and reaction energies are efficiently transferred into translational mode and the C−F stretching mode of CH_3F, whereas it is not transferred into C−H stretching mode. This is because vibrational mode couplings between the C−H and C−F modes are negligibly weak in the course of the S_N2 reaction. This feature is also obtained by Hase's classical trajectory calculations.[3] On the other hand, in the case of S_N2 reaction of OH^-, the O−C stretching energy of CH_3OH is efficiently transferred into the C−H stretching mode via the vibrational coupling with the O−H stretching mode. This energy transfer causes the vibrational mode excitation of the C−H stretching of CH_3OH. This feature obtained in the reaction of OH^- is much different from those of the other S_N2 reactions of atomic ion X^-. This is the unique feature in the present system. Unfortunately, the product state distribution in the title reaction was not measured experimentally yet. However, it will likely be detected by developing experimental techniques soon.

Recently, accurate potential energy diagrams for reaction I have obtained by Se and Morokuma.[17] Their calculations at the CCSD(T)/aug-cc-pVDZ//MP2/aug-cc-pVDZ level indicated that the energy level of the transition state for reaction I is lower than that of the initial separation (the energy is calculated to be −13.4 kcal/mol), which is in good agreement with the present calculation (−16.5 kcal/mol) at the HF/3-21+G(d) level. Also, the structures at the stationary points agreed well with the present calculations.

C. Concluding Remarks. We have introduced several approximations to calculate the potential energy surface and to treat the reaction dynamics. First, we assumed HF/3-21+G(d) multidimensional potential energy surface in the trajectory calculations throughout. As shown in section 3.1, the shape of PES for the $OH^- + CH_3Cl$ reaction system calculated at the HF/3-21+G(d) level of theory is in good agreement with that of MP2/6-311++G(2df,2pd) level. Therefore, it is enough to discuss at least qualitatively the reaction dynamics for the $OH^- + CH_3Cl$ reaction system. However, more accurate wave function and accurate method may provide deeper insight into the dynamics. Second, we calculated 73 trajectories for each collision energy ($E_{coll} = 5.0$ and 25.0 kcal/mol). In addition, almost all trajectories were calculated with near-zero impact parameters. The number of trajectories in the present work may be enough to discuss at least the qualitative features of the dynamics. However, a large number of trajectories with larger impact parameters are needed to obtain more accurate reaction rate. Despite the several assumptions introduced here, the results enable us to obtain valuable information on the mechanism of the microsolvated S_N2 reaction. The trajectory calculations as the random collisions are now in progress.[27]

Acknowledgment. The authors are indebted to the Computer Center at the Institute for Molecular Science (IMS) for the use of the computing facilities. One of the authors (H.T.) also acknowledges a partial support from a Grant-in-Aid for Scientific Research (C) from the Japan Society for the Promotion of Science (JSPS).

References and Notes

(1) For a selection of experimental works on gas-phase S_N2 reaction, see: (a) Olmstead, W. N.; Brauman, J. I. *J. Am. Chem. Soc.* **1977**, *99*, 44219. (b) Su, T.; Morris, R. A.; Viggiano, A. A.; Paulson, J. F. *J. Phys. Chem.* **1990**, *94*, 8426. (c) Viggiano, A. A.; Paschkewitz, J. S.; Morris, R. A.; Paulson, J. F.; Gonzalez-Lafont, A.; Truhlar, D. G. *J. Am. Chem. Soc.* **1991**, *113*, 9404. (d) DePuy, C. H.; Gronert, S.; Mullin, A.; Bierbaum, V. M. *J. Am. Chem. Soc.* **1990**, *112*, 8650. (e) Gronert, S.; DePuy, C. H.; Bierbaum, V. M. *J. Am. Chem. Soc.* **1991**, *113*, 4009. (f) Graul, S. T.; Bowers, M. T. *J. Am. Chem. Soc.* **1991**, *113*, 9696. (g) Graul, S. T.; Bowers, M. T. *J. Am. Chem. Soc.* **1994**, *116*, 3875. (h) Van Orden, S. L.; Pope, R. M.; Buckner, S. W. *Org. Mass Spectrom.* **1991**, *26*, 1003. (i) Cyr, D. M.; Posey, L. A.; Bishea, G. A.; Han, C.-C.; Johnson, M. A. *J. Am. Chem. Soc.* **1991**, *113*, 9697. (j) Cyr, D. M.; Bishea, G. A.; Scarton, M. G.; Johnson, M. A. *J. Chem. Phys.* **1992**, *97*, 5911. (k) Giles, K.; Grimsrud, E. P. *J. Phys. Chem.* **1992**, *96*, 6680. Knighton, W. B.; Boghar, J. A.; O'Connor, P. M.; Grimsrud, E. P. *J. Am. Chem. Soc.* **1993**, *115*, 12079. (l) Sahlstrom, K. E.; Knighton, W. B.; Grimsrud, E. P. *J. Phys. Chem. A* **1997**, *101*, 1501. (m) Viggiano, A. A.; Morris, R. A.; Paschkewitz, J. S.; Paulson, J. F. *J. Am. Chem. Soc.* **1992**, *114*, 10477. (n) Wladkowski, B. D.; Lim, K. F.; Allen, W. D.; Brauman, J. I. *J. Am. Chem. Soc.* **1992**, *114*, 9136. (o) Viggiano, A. A.; Morris, R. A.; Su, T.; Wladkowski, B. D.; Craig, S. L.; Zhong, M.; Brauman, J. I. *J. Am. Chem. Soc.* **1994**, *116*, 2213. (p) Craig, S. L.; Brauman, J. I. *Science* **1997**, *276*, 1536. (q) Viggiano, A. A.; Morris, R. A. *J. Phys. Chem.* **1994**, *98*, 3740. (r) Li, C.; Ross, P.; Szulejko, J. E.; McMahon, T. B. *J. Am. Chem. Soc.* **1996**, *118*, 9360. (s) Craig, S. L.; Brauman, J. I. *J. Phys. Chem. A* **1997**, *101*, 4745. (t) DeTuri, V. F.; Hintz, P. A.; Ervin, K. M. *J. Phys. Chem. A* **1997**, *101*, 5969. (u) Seeley, J. V.; Morris, R. A.; Viggiano, A. A.; Wang, H.; Hase, W. L. *J. Am. Chem. Soc.* **1997**, *119*, 577. (v) Le Garrec, J.-L.; Rowe, B. R.; Queffelec, J. L.; Mitchell, J. B. A.; Clary, D. C. *J. Chem. Phys.* **1997**, *107*, 1021. (w) Chabinyc, M. L.; Craig, S. L.; Regan, C. K.; Brauman, J. I. *Science* **1998**, *279*, 1882. (x) Hierl, P. M.; Paulson, J. F.; Henchman, M. J. *J. Phys. Chem.* **1995**, *99*, 15655.

(2) For a selection of theoretical studies of S_N2 reactions, see: (a) Ryaboy, V. M. In *Advances in Classical Trajectory Methods*; Hase, W. L., Ed.; JAI Press: Greenwich, CT, 1994; Vol. 2, pp 115−145. (b) Vande Linde, S. R.; Hase, W. L. *J. Phys. Chem.* **1990**, *94*, 2778. (c) Tucker, S. C.; Truhlar, D. G. *J. Am. Chem. Soc.* **1990**, *112*, 3338. (d) Billing, G. D. *Chem. Phys.* **1992**, *159*, 109. (e) Wladkowski, B. D.; Allen, W. D.; Brauman, J. I. *J. Phys. Chem.* **1994**, *98*, 13532. (f) Wang, H.; Zhu, L.; Hase, W. L. *J. Phys. Chem.* **1994**, *98*, 1608. (g) Wang, H.; Hase, W. L. *J. Am. Chem. Soc.* **1995**, *117*, 9347. (h) Hu, W.-P.; Truhlar, D. G. *J. Am. Chem. Soc.* **1995**, *117*, 10726. (i) Glukhovtsev, M. N.; Pross, A.; Radom, L. *J. Am. Chem. Soc.* **1995**, *117*, 2024. (j) Glukhovtsev, M. N.; Pross, A.; Radom, L. *J. Am. Chem. Soc.* **1996**, *118*, 6273. (k) Wang, H.; Hase, W. L. *Chem. Phys.* **1996**, *212*, 247. (l) Clary, D. C.; Palma, J. *J. Chem. Phys.* **1996**, *106*, 575. (m) Wang, H.; Goldfield, E. M.; Hase, W. L. *J. Chem. Soc., Faraday Trans.* **1997**, *93*, 737. (n) Botschwina, P.; Horn, M.; Seeger, S.; Oswald, R. *Ber. Bunsen-Ges. Phys. Chem.* **1997**, *101*, 387. (o) Baer, T.; Hase, W. L. *Unimolecular Reaction Dynamics-Theory and Experiments*; Oxford: New York, 1996.

(3) . Trajectory studies for the S_N2 reaction: (a) Vande Linde, S. R.; Hase, W. L. *J. Phys. Chem.* **1990**, *94*, 6148. (b) Vande Linde, S. R.; Hase,

W. L. *J. Chem. Phys*. **1990**, *93*, 7962. (c) Peslherbe, G. H.; Wang, H.; Hase, W. L. *J. Chem. Phys*. **1995**, *102*, 5626. (d) Cho, Y. J.; Vande Linde, S. R.; Zhu, L.; Hase, W. L. *J. Chem. Phys*. **1992**, *96*, 8275. (e) Hase, W. L.; Cho, Y. J. *J. Chem. Phys*. **1993**, *98*, 8626. (f) Wang, H.; Peslherbe, G. H.; Hase, W. L. *J. Am. Chem. Soc*. **1994**, *116*, 9644. (g) Peslherbe, G. H.; Wang, H.; Hase, W. L. *J. Am. Chem. Soc*. **1996**, *118*, 2257. (h) Hase, W. L. *Science* **1994**, *266*, 998. (i) Wang, H.; Hase, W. L. *Int. J. Mass Spectrom. Ion Process*. **1997**, *167*, 573, 22. (j) Li, G.; Hase, W. L. *J. Am. Chem. Soc*. **1999**, *121*, 7124. (k) Wang, H.; Hase, W. L. *J. Am. Chem. Soc*. **1997**, *119*, 3093. (l) Craig, S. L.; Brauman, J. I. *J. Phys. Chem. A* **1997**, *101*, 4745. (m) Sun, L.; Hase, W. L.; Song, K. *J. Am. Chem. Soc*. **2001**, *123*, 5753.

(4) For a selection of quantum scattering studies for the S_N2 reaction, see: (a) Clary, D. C.; Palma, J. *J. Chem. Phys*. **1997**, *106*, 575. (b) Schmatz, S.; Clary, D. C. J. *Chem. Phys*. **1999**, *110*, 9483. (c) Hernandez, M. I.; Campos-Martinez, J.; Villarreal, P.; Schmatz, S.; Clary, D. C. *Phys. Chem. Chem. Phys*. **1999**, *1*, 1197.

(5) Tachikawa, H. *J. Phys. Chem. A* **2001**, *105*, 1260.

(6) Tachikawa, H. *J. Phys. Chem. A* **2000**, *104*, 497.

(7) Tachikawa, H.; Igarashi, M. *Chem. Phys. Lett*. **1999**, *303*, 81.

(8) Igarashi, M.; Tachikawa, H. *Int. J. Mass Spectrom*. **1998**, *181*, 151.

(9) Paulson, J. F.; Dale, F. *J. Chem. Phys*. **1982**, *77*, 4006.

(10) Henchman, M.; Paulson, J. F.; Hierl, P. M. *J. Am. Chem. Soc*. **1983**, *105*, 5509.

(11) Paulson, J. F. *J. Chem. Phys*. **1970**, *52*, 959.

(12) Bohme, D. K.; Raksit, A. B. *J. Am. Chem. Soc*. **1984**, *106*, 3447.

(13) Tanaka, K.; Mackay, G. I.; Payzant, I. D.; Bohme, D. K. *Can. J. Chem*. **1976**, *54*, 1643.

(14) Olmstread, W. N.; Brauman, J. I. *J. Am. Chem. Soc*. **1977**, *99*, 4219.

(15) Hierl, P. M.; Ahrens, A. F.; Henchman, M.; Viggiano, A. A.; Paulson, J. F.; Clary, D. C. *J. Am. Chem. Soc*. **1986**, *108*, 3142.

(16) Ohta, K.; Morokuma, K. *J. Phys. Chem*. **1985**, *89*, 5845.

(17) Re, S.; Morokuma, K. *J. Phys. Chem. A* **2001**, *105*, 7185.

(18) Evanseck, J. D.; Blake, J. F.; Jorgensen, W. L. *J. Am. Chem. Soc*. **1987**, *109*, 2349.

(19) Gonzales, J. M.; Cox, R. S.; Brown, S. T.; Allen, W. D.; Schaefer, H. F. *J. Phys. Chem. A* **2001**, *105*, 11327.

(20) Frisch, M. J.; Trucks, G. W.; Schlegel, H. B.; Scuseria, G. E.; Robb, M. A.; Cheeseman, J. R.; Zakrzewski, V. G.; Montgomery, J. A., Jr.; Stratmann, R. E.; Burant, J. C.; Dapprich, S.; Millam, J. M.; Daniels, A. D.; Kudin, K. N.; Strain, M. C.; Farkas, O.; Tomasi, J.; Barone, V.; Cossi, M.; Cammi, R.; Mennucci, B.; Pomelli, C.; Adamo, C.; Clifford, S.; Ochterski, J.; Petersson, G. A.; Ayala, P. Y.; Cui, Q.; Morokuma, K.; Malick, D. K.; Rabuck, A. D.; Raghavachari, K.; Foresman, J. B.; Cioslowski, J.; Ortiz, J. V.; Stefanov, B. B.; Liu, G.; Liashenko, A.; Piskorz, P.; Komaromi, I.; Gomperts, R.; Martin, R. L.; Fox, D. J.; Keith, T.; Al-Laham, M. A.; Peng, C. Y.; Nanayakkara, A.; Gonzalez, C.; Challacombe, M.; Gill, P. M. W.; Johnson, B. G.; Chen, W.; Wong, M. W.; Andres, J. L.; Head-Gordon, M.; Replogle, E. S.; Pople, J. A. *Gaussian 98*, revision A.5; Gaussian, Inc.: Pittsburgh, PA, 1998.

(21) Vreven, T.; Bernardi, F.; Garavelli, M.; Olivucci M.; Robb, M. A.; Schlegel, H. B. *J. Am. Chem. Soc*. **1997**, *119*, 12687.

(22) (a) Chen, W.; Hase, W. L.; Schlegel, H. B. *Chem. Phys. Lett*. **1994**, *228*, 436. (b) Li, G. S.; Hase, W. L. *J. Am. Chem. Soc*. **1999**, *121*, 7124.

(23) Helgaker, E.; Uggerud, H.; Jonsen, H. J. A. *Chem. Phys. Lett*. **1990**, *173*, 145.

(24) Tachikawa, H. *J. Phys. Chem. A* **2000**, *104*, 7738.

(25) Tachikawa, H. *Phys. Chem. Chem. Phys*. **2000**, *2*, 839.

(26) Henchman, M.; Paulson, J. F.; Hierl, P. M. *J. Am. Chem. Soc*. **1983**, *105*, 5509.

(27) Tachikawa, H.; Igarashi, M.; Ishibashi, T., to be submitted for publication.

(28) Shimanouchi, T. Molecular vibrational Frequencies. In *NIST Chemistry WebBook*; Linstrom, P. J., Mallard, W. G., Eds.; NIST Standard Reference Database Number 69; National Institute of Standards and Technology: Gaithersburg, MD, July 2001 (http://webbook.nist.gov).